Advances in Nano Research, *Vol. 13, No.5 (2022) 475-485*
https://doi.org/10.12989/anr.2022.13.5.475

Enhance photoelectric efficiency of PV by optical-thermal management of nanofilm reflector

Huaxu Liang[1], Baisheng Wang[2,3], Ronghua Su[4], Ao Zhang[4], Fuqiang Wang[*1,2] and Yong Shuai[1]

[1]*School of Energy Science and Engineering, Harbin Institute of Technology, 92, West Dazhi Street, Harbin 150001, PR China*
[2]*School of New Energy, Harbin Institute of Technology at Weihai, 2, West Wenhua Road, Weihai 264209, PR China*
[3]*Xuzhou Xugong Road Construction Machinery Co., Ltd, 10, tuolanshan Road, Xuzhou City 221001, PR China*
[4]*Institute of Defense Engineering, Academy of Military Science, PLA, Beijing 100850 PR China*

(*Received November 21, 2021, Revised July 12, 2022, Accepted July 13, 2022*)

Abstract. Crystalline silicon photovoltaic cells have advantages of zero pollution, large scale and high reliability. A major challenge is that sunlight wavelength with photon energy lower than semiconductor band gap is converted into heat and increase its temperature and reduce its conversion efficiency. Traditional cooling PV method is using water flowing below the modules to cool down PV temperature. In this paper, the idea is proposed to reduce the temperature of the module and improve the energy conversion efficiency of the module through the modulation of the solar spectrum. A spectrally selective nanofilm reflector located directly on the surface of PV is designed, which can reflect sunlight wavelength with low photon energy, and even enhance absorption of sunlight wavelength with high photon energy. The results indicate that nanofilm reflector can reduce spectral reflectivity integral from 9.0% to 6.93% in 400~1100 nm wavelength range, and improve spectral reflectivity integral from 23.1% to 78.34% in long wavelength range. The nanofilm reflector can reduce temperature of PV by 4.51℃ and relatively improved energy conversion efficiency of PV by 1.25% when solar irradiance is 1000 W/m². Furthermore, the nanofilm reflector is insensitive in sunlight's angle and polarization state, and be suitable for high irradiance environment.
Keywords: crystalline silicon photovoltaic cells; nanofilm; radiative transfer; solar energy; spectral splitting

1. Introduction

The efficient utilization of solar energy is an effective way to replace fossil energy and serve carbon neutrality strategy (Arıcı *et al*. 2020, Lee and Lee 2018). In the recent years, many efforts have been done for improving the energy conversion of solar energy (Cheng *et al*. 2021, Mateusz *et al*. 2018). Photovoltaic (PV) conversion, photothermal conversion, and photochemical conversion are three common methods utilizing solar energy (Evangelos *et al*. 2021). Among above three types of solar energy utilization methods, many efforts have been made to convert full spectrum solar energy into thermal energy (Muhammad *et al*. 2019, Hu *et al*. 2022). However, photoelectric conversion can convert solar energy to electricity (Kruitwagen *et al*. 2021), which has grown fast and reached the global cumulative installed capacity of 756 GWp by the end of 2020. Crystalline silicon photovoltaic cells occupy 95% of the global PV market due to its highly efficient and stable operation. Crystalline silicon photovoltaic cells are a promising method to serve carbon neutrality strategy (Zarmai *et al*. 2015).

Crystalline silicon photovoltaic cells are semiconductor devices, which means that they can only convert certain part of full spectrum solar energy to electricity (Fernandes and Schaefer 2021). The sunlight wavelength with photon energy high than the semiconductor band gap can be converted to electricity (Klaus *et al*. 2021). However, the sunlight wavelength with photon energy lower than the semiconductor band gap is absorbed by free-carriers, as presented in Fig. 1(a), which is converted to wasted heat (Michel *et al*. 2017). The wasted heat increases the temperature of crystalline silicon photovoltaic cells. Every 1K increase in temperature would reduce the efficiency of a crystalline silicon photovoltaic cells by ~0.4% (Haviv *et al*. 2020).

To remove excess heat of crystalline silicon photovoltaic cells, the photovoltaic/thermal (PV/T) system was studied (Caselli *et al*. 2014, Liang *et al*. 2021). In such system, a cooling fluid is flowing below module and absorbing thermal energy from module (Ju *et al*. 2017). Many researches have studied and enhanced the performance of PV/T system by optimizing optical design, geometrical design and operating parameters (Hissouf *et al*. 2021). However, such PV/T system increases the cost of mechanical components, power, and subsequent maintenance.

On the other hand, the spectral splitting photovoltaic/thermal system has gained great interesting. Two types spectral splitting photovoltaic/thermal system like nanofluid based spectral splitting photovoltaic/thermal system and nanofilm based spectral splitting photovoltaic/thermal system are studied intensively (Li *et al*. 2019, Daulet 2021). Farideh *et al*. (2020) use nanofluids to pre-absorb sunlight wavelength with photon energy lower than the semi-conductor band gap and transmit sunlight wavelength with photon energy higher than the semiconductor band gap to

*Corresponding author, Professor,
E-mail: wangfuqiang@hitwh.edu.cn

ISSN: 2287-237X (Print), 2287-2388 (Online)

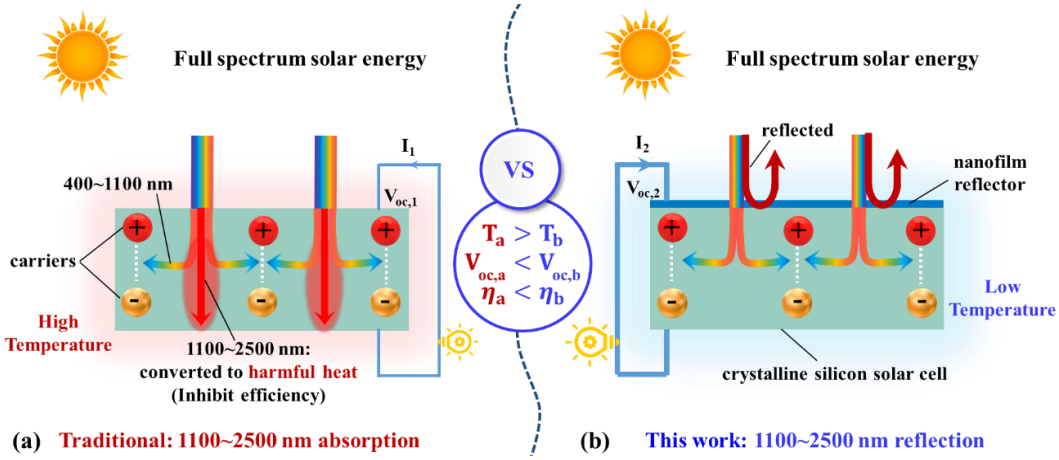

Fig. 1 (a) the sunlight wavelength with photon energy lower than the semiconductor band gap is absorbed by crystalline silicon photovoltaic cells, which is converted to heat and reduces its conversion efficiency; (b) the sunlight wavelength with photon energy lower than the semiconductor band gap is reflected when spectrally selective nanofilm reflector is placed on the surface of crystalline silicon photovoltaic cells, which can improve its conversion efficiency

the crystalline silicon photovoltaic cells. And stabilizer has been created to make nanoparticles more stable by Qiao *et al*. (2021). Zhang *et al*. (2022) proposed a flexible control strategy for controlling the temperature nanofluid of such nanofluid based spectral splitting photovoltaic/thermal system, which could satisfy the requirement of radiant floor heating. Huang *et al*. (2021) used 25.4 mg/L Ag@SiO_2/$CoSO_4$-PG nanofluid as a nofluid filter, which can produce total solar energy conversion efficiency of 63.3% and yield economic value enhancement of 67.8% compared to the PV only system. Other types of nanofluids (Otanicar *et al*. 2018, Ravi *et al*. 2021), have also been investigated. However, the nanofluid additionally absorb part of sunlight wavelength with photon energy higher than the semiconductor band gap, which is not available in practice (Liang *et al*. 2020). Other scholars use nanofilm-based spectral splitting devices to reflect short wavelengths with photon energies larger than the semiconductor band gap to the solar cell and direct long wavelengths with photon energies smaller than the semiconductor band gap to the thermal absorber (Huang and Markides 2021). Zhang *et al*. (2021) fabricated a novel double-layer SiN_x/Cu SBS film by magnetron sputtering, which could have a high transmittance of 72.9% and a reflectance of 89.7%. Many studies have indicated that nanofluids and nanofilm-based spectral splitting devices can be used to decrease the temperature of photovoltaic cells (Robert *et al*. 2012). However, the application of these spectral splitting photovoltaic/thermal system is restricted by: (1) precise optical path requirements that, if unmet, can lead to serious light leakage; (2) high optical loss due to the multiple light paths between multiple optical devices, such as nanofluids and nanofilm-based spectral splitting devices; (3) the expensive fabricated fee of nanofilm-based spectral splitting devices and the instability of nanofluid.

In this paper, the idea of using nanofilm reflector to reduce the temperature of photovoltaic cells is proposed, which overcomes the limitation of high optical loss and precise optical path requirements existing in traditional cooling method based on solar spectrum regulation. Such nanofilm reflector is located on the surface of crystalline silicon photovoltaic cells to reflect sunlight wavelength with photon energy lower than the semiconductor band gap, as presented in Fig. 1(b). In addition, such nanofilm reflector would not reflect sunlight wavelength with photon energy higher than the semiconductor band gap additionally, which could maintain or even enhance the anti-reflection performance in 400~1100 nm for crystalline silicon photovoltaic cell. The nanofilm reflector is multilayer nanofilm structure, which is globally optimized in material, number of layers and thickness of layers. The effects of incident angle and polarization on the optical performance of crystalline silicon photovoltaic cells with nanofilm reflector is studied. The temperature of crystalline silicon photovoltaic cells with nanofilm reflector is compared to that of crystalline silicon photovoltaic cells without nanofilm reflector. The energy conversion efficiency of the crystalline silicon photovoltaic cells with nanofilm reflector is compared to that of crystalline silicon photovoltaic cells without nanofilm reflector.

Fig. 1(a) the sunlight wavelength with photon energy lower than the semiconductor band gap is absorbed by crystalline silicon photovoltaic cells, which is converted to heat and reduces its conversion efficiency; (b) the sunlight wavelength with photon energy lower than the semiconductor band gap is reflected when spectrally selective nanofilm reflector is placed on the surface of crystalline silicon photovoltaic cells, which can improve its conversion efficiency.

2. Methodology

2.1 Design of nanofilm reflector for crystalline silicon photovoltaic cells

The spectral absorption of crystalline silicon photovoltaic cells is presented in Fig. 2(a) (Santbergen and

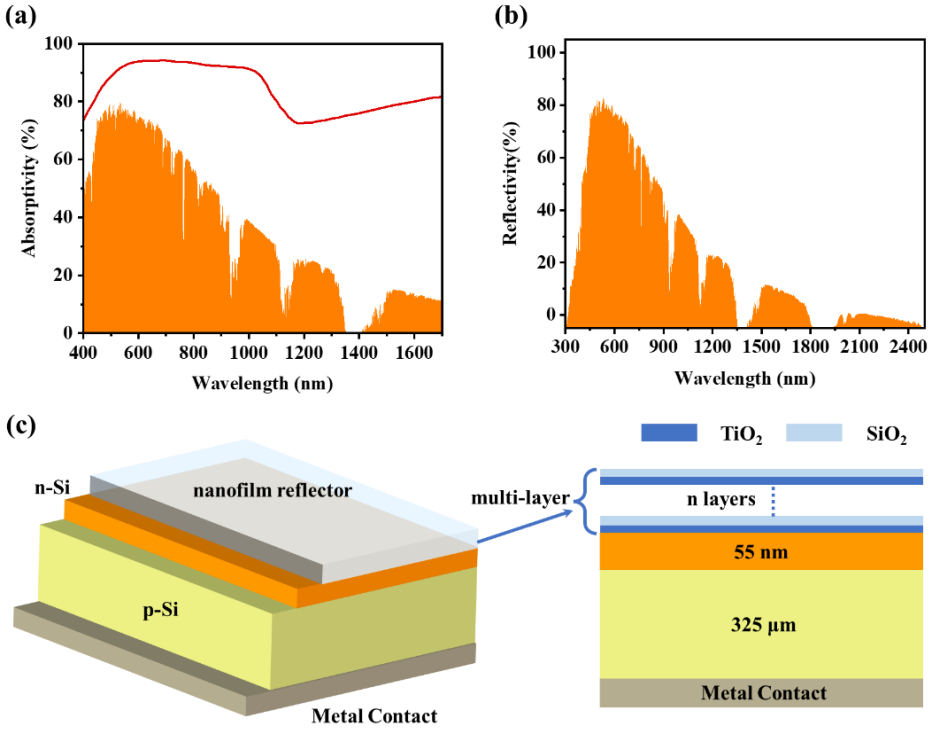

Fig. 2 (a) the spectral absorption of crystalline silicon photovoltaic cells; (b) the ideal optical property of the nanofilm reflector, which should have low reflectivity in the 400~1100 nm and high reflectivity in the 1100~2500 nm; (c) the design model of nanofilm reflector placing on the surface of crystalline silicon photovoltaic cells

Zolingen 2008) The crystalline silicon photovoltaic cells have a high absorption in the 400~1100 nm, since the silicon band gap is about 1.1ev. It should be noted that the intrinsic silicon is transparent at the wavelength range from 1100 nm to 1700 nm, however, the doping silicon is not transparent at the wavelength range from 1100 nm to 1700 nm. The free-carrier absorption coefficient is a function of doping concentration. The maximum n-type doping concentration in the emitter typically is $3.3 \times 10^{20} cm^{-3}$. The crystalline silicon photovoltaic cells also have a high absorption in the 1100~1700 nm with photon energy lower than the silicon band gap. Such absorption of 1100~1700 nm with photon energy lower than the silicon band gap is caused by free-carrier in doped regions (Green 1995). Such absorption of 1100~1700 nm with photon energy lower than the silicon band gap is about $100W/m^2$, which is converted to heat rather than electricity.

In order to prevent the 1100~1700 nm sunlight wavelength absorbed by the crystalline silicon photovoltaic cells, a nanofilm reflector with high selective reflectivity is put on the top surface of the crystalline silicon photovoltaic cells. As presented in Fig. 2(b), the nanofilm reflector should have low reflectivity in the 400~1100 nm to reduce the reflection loss, which could make the crystalline silicon photovoltaic cells generate as much electricity as possible. The nanofilm reflector also should have high reflectivity in the 1100~2500 nm to improve the reflection, so as to reduce the temperature of the crystalline silicon photovoltaic cell as much as possible.

The nanofilm reflector with high selective reflectivity is put on the surface of the crystalline silicon photovoltaic cells, as presented in Fig. 2(c). In particular, silicon's band gap is slightly too low, it has a low absorption coefficient. While the low absorption coefficient can be overcome by light trapping, silicon is also difficult to grow into thin sheets. Therefore, thickness between 200 and 500μm are typically used for silicon solar cell. In this study, the p type layer is selected as 325μm. In addition, N type layer has a higher surface quality than p-type silicon so it is placed at the front of the cell where most of the light is absorbed. By making the front layer very thin, a large fraction of the carriers generated by the incoming light are created within a diffusion length of the p-n junction. Therefore, in this study, the n layer is selected as 55nm. The nanofilm reflector is multilayer nanofilm structure (Taylor *et al*. 2020). The materials of the multilayer nanofilm must be transparent, large index mismatch over the 400~2500 nm. The materials of the multilayer nanofilm also needs to be inexpensive. Therefore, the materials of TiO_2 and SiO_2 are used in this paper.

Table 1 Layer thickness of 2-layer film

Layer number	1	2
Material	TiO_2	SiO_2
Thickness (nm)	95	57

Table 2 Layer thickness of 4-layer film

Layer number	1	2	3	4
Material	TiO_2	SiO_2	TiO_2	SiO_2
Thickness (nm)	72	37	10	38

Table 3 Layer thickness of 14-layer film

Layer number	1	2	3	4	5	6	7
Material	TiO_2	SiO_2	TiO_2	SiO_2	TiO_2	SiO_2	TiO_2
Thickness (nm)	57	239	11	36	154	27	15
Layer number	8	9	10	11	12	13	14
Material	SiO_2	TiO_2	SiO_2	TiO_2	SiO_2	TiO_2	SiO_2
Thickness (nm)	246	18	22	142	13	17	88

Table 4 Layer thickness of 26-layer film

Layer number	1	2	3	4	5	6	7
Material	TiO_2	SiO_2	TiO_2	SiO_2	TiO_2	SiO_2	TiO_2
Thickness (nm)	64	40	10	182	12	34	138
Layer number	8	9	10	11	12	13	14
Material	SiO_2	TiO_2	SiO_2	TiO_2	SiO_2	TiO_2	SiO_2
Thickness (nm)	29	15	230	14	23	152	10
Layer number	15	16	17	18	19	20	21
Material	TiO_2	SiO_2	TiO_2	SiO_2	TiO_2	SiO_2	TiO_2
Thickness (nm)	28	42	10	227	12	33	25
Layer number	22	23	24	25	26		
Material	SiO_2	TiO_2	SiO_2	TiO_2	SiO_2		
Thickness (nm)	11	124	14	25	92		

Table 5 Layer thickness of 30-layer film

Layer number	1	2	3	4	5	6
Material	TiO_2	SiO_2	TiO_2	SiO_2	TiO_2	SiO_2
Thickness (nm)	58	206	18	24	125	21
Layer number	7	8	9	10	11	12
Material	TiO_2	SiO_2	TiO_2	SiO_2	TiO_2	SiO_2
Thickness (nm)	16	207	18	19	139	23
Layer number	13	14	15	16	17	18
Material	TiO_2	SiO_2	TiO_2	SiO_2	TiO_2	SiO_2
Thickness (nm)	14	240	16	30	152	18
Layer number	19	20	21	22	23	24
Material	TiO_2	SiO_2	TiO_2	SiO_2	TiO_2	SiO_2
Thickness (nm)	34	56	10	281	15	41
Layer number	25	26	27	28	29	30
Material	TiO_2	SiO_2	TiO_2	SiO_2	TiO_2	SiO_2
Thickness (nm)	31	10	125	12	29	96

2.2 Calculating the optical property of nanofilm reflector

A high refractive index (n_1) film with an optical thickness of $\lambda_0/4$ is plated on a substrate with a refractive index of n_g, the reflectivity is calculated as:

$$R = \left(\frac{n_0 - n_1^2/n_g}{n_0 + n_1^2/n_g} \right)^2 \quad (1)$$

where n_0 is the refractive index of air, n_1^2/n_g is the admittance of monolayer film and substrate combination.

In practice, the refractive index (n_1) of the film is limited, and the highest reflectance achievable by a single-layer film will not exceed 50%.

If a dielectric multilayer film with the thickness of each layer being $\lambda_0/4$ and alternating high and low refractive indexes is used, a better reflectivity can be obtained. This is because the light beams reflected from all interfaces of the film have the same phase when they return to the front surface, resulting in constructive interference, and achieving high reflectivity.

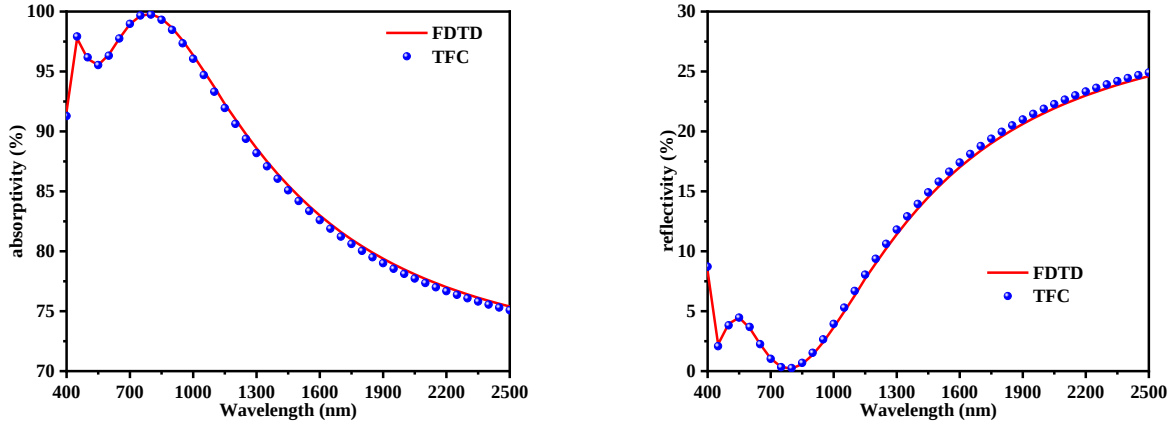

(a) (b)

Fig. 3(a) the spectral absorptivity calculated by TFC method using in this paper match well with those calculated using the FDTD method; (b) the spectral reflectivity calculated by TFC method using in this paper match well with those calculated using the FDTD method

In this paper, a series of stacks with $G(HL)_N A$ is adopted to obtain the preliminary selective reflectivity. Then the needle method will be used to optimize the stacks and obtain the excepted selective reflectivity. The working principle of the needle optimization method is to increase a new layer to the stacks and use the local optimization method to optimize the new stacks, which is implemented in the thin film design software TFCalc (Khan *et al*. 2020, Tikhonravov *et al*. 1996). The optimized structure parameters are listed in Tables 1-5.

2.3 Calculating the energy conversion efficiency

The average absorption (A) of PV is:

$$A = \frac{\int A_\lambda S_\lambda d\lambda}{\int S_\lambda d\lambda} \tag{2}$$

where S_λ is the Solar irradiance spectrum at AM1.5, A_λ is the spectral absorptivity of the PV.

According to the literature, it can be known that the spectral absorptivity of crystalline silicon photovoltaic cells without nanofilm reflector in the 400-1700 nm band is between 0.7-1. In this study, the spectral absorptivity of crystalline silicon photovoltaic cells without nanofilm reflector in the 1700-2500nm band is assumed as 0.7. Currently, some PV manufacturers place the grid lines underneath, and there are no grid lines on the front of the PV, the thermal conversion efficiency (A_{eff}) of PV is:

$$A_{eff} = A - \eta_{el}(T_{cell}) \tag{3}$$

where η_{el} is the energy conversion efficiency of the PV.

The temperature difference is (Santbergen and Zolingen, 2008):

$$T_{cell} - T_{amb} = \kappa A_{eff} G \tag{4}$$

where T_{cell} is the temperature of the PV, T_{amb} is the ambient temperature (25°C), G is the solar irradiance, and κ =0.043°C/(W/m^2) (Santbergen and Zolingen 2008).

The efficiency of photovoltaic cells at actual temperature $\eta_{el}(T_{cell})$ is:

$$\eta_{el}(T_{cell}) = \eta_{el}^{STC}\left\{1+\beta\left(T_{cell}-25℃\right)\right\} \tag{5}$$

where η_{el}^{STC} is the photoelectric conversion efficiency of photovoltaic cells tested under standard condition. β is temperature conversion factor of PV, β = -0.45%/°C.

3. Model validation

In order to validate the model results in this study, the calculated spectral absorptivity and reflectivity are compared with the results obtained by solving the Maxwell's equations, since the light transport can be solved by the Maxwell's equation (Qiu *et al*. 2021). The model for the validation is the Si/TiO_2/SiO_2 tandem structure. The thickness of the Si, TiO_2 and SiO_2 are 0.5mm, 58 nm and 94 nm, respectively. The calculated spectral absorptivity and reflectivity are compared with the results obtained by finite-difference time-domain (FDTD) method, as presented in Fig. 3. As presented in the graph, the spectral absorptivity and reflectivity calculated by TFC method in this paper match well with those calculated using the FDTD method. The maximum absolute error between the two methods ($\delta_{\max} = |A_{\mathrm{TFC}} - A_{\mathrm{FDTD}}|$) was less than 1%. According to the above two cases, it can be summarized that the method used in this study can achieve accurate calculation precision.

4. Results and discussion

4.1 Spectral reflectivity comparison

To investigate the possibility of placing nanofilm

reflector on the existing crystalline silicon photovoltaic cells from the perspective of optical properties, the reflectivity of the crystalline silicon photovoltaic cells with nanofilm reflector is compared with that of the crystalline silicon photovoltaic cells without nanofilm reflector (Santbergen and Zolingen 2008). The structure of the crystalline silicon photovoltaic cells with nanofilm reflector is Ag/p-Si/n-Si/TiO_2/SiO_2 tandem structure. The thickness of p-Si layer is 325μm, the thickness of n-Si layer is 55 nm, which is same as the structure parameters in Ref (Santbergen and Zolingen 2008). The thickness of TiO_2 and SiO_2 layers are 95 nm and 57nm, respectively.

The spectral reflectivity of the crystalline silicon photovoltaic cell with/without nanofilm reflector are presented in Fig. 4. As shown in the figure, the reflectivity of the crystalline silicon photovoltaic cell with nanofilm reflector is above 0.7 in the 1100~1700 nm wavelength range, while the reflectivity of the crystalline silicon photovoltaic cell without nanofilm reflector is below 0.3 in the 1100~1700 nm wavelength range. Therefore, the crystalline silicon photovoltaic cell with nanofilm reflector exhibits a larger reflection in the 1100~1700 nm wavelength range, which indicated that the nanofilm reflector can prevent the sub-absorption of the crystalline silicon photovoltaic cell that generating heat. In addition, the reflectivity of the crystalline silicon photovoltaic cell with nanofilm reflector is below 0.05 in the 400~1100 nm wavelength range, while the reflectivity of the crystalline silicon photovoltaic cell without nanofilm reflector is above 0.05 in the 400~1100 nm wavelength range. In summary, our designed nanofilm reflector has very good anti-reflection performance, and can reduce the absorption of 1100~1700 nm by crystalline silicon photovoltaic cell as much as possible.

Therefore, the crystalline silicon photovoltaic cell with nanofilm reflector exhibits a lower reflection in the 400~1100 nm wavelength range, which indicated that the nanofilm reflector has anti-reflection effect to improve the band to band absorption of the crystalline silicon photovoltaic cell for generating electricity. In the 400~1100 nm wavelength range, the spectral reflectivity integral ($R_{400\sim1100nm}$) of crystalline silicon photovoltaic cell with nanofilm reflector is 6.93%, which is lower than that of the crystalline silicon photovoltaic cell without nanofilm reflector with the $R_{400\sim1100nm}$ of 9.0%. In 1100~1700 nm wavelength range, spectral reflectivity integral ($R_{400\sim1700nm}$) of crystalline silicon photovoltaic cell with nanofilm reflector is 78.34%, which is higher than that of photovoltaic cell without nanofilm reflector with $R_{400\sim1700nm}$ of 23.1%. Therefore, nanofilm reflector can suppress sub-absorption and improve band to band absorption.

4.2 Angular and polarization study

The nanofilm reflector with two layers of TiO_2/SiO_2 can suppress the sub-absorption and improve the band to band absorption for the sunlight incident normal to surface of crystalline silicon photovoltaic cell. However, for practical crystalline silicon photovoltaic cell applications, the incident sunlight is not normal to surface of the crystalline silicon photovoltaic cell all the time. For example, 85° irradiation will occur when day and night alternate, and surrounding objects will scatter light to the PV with an oblique incidence angle. It is important to ensure that nanofilm reflector can capture the sunlight with different incident angles (Cote *et al*. 2021, Slauch *et al*. 2018). In addition, if the incident sunlight is oblique, the polarization of incident light has an effect on the optical performance of the nanofilm reflector. For normal incident light, the reflectivity of TE (transverse electrical) polarized state is same as that of TM (transverse magnetic) polarized state, while for the oblique incident light, the reflectivity of TE polarized state is not same as that of TM polarized state. Therefore, in this section, the effects of incident angle and polarization on the optical performance of the crystalline silicon photovoltaic cell with two layers of TiO_2/SiO_2 nanofilm reflector are investigated, as presented in Fig. 5(a).

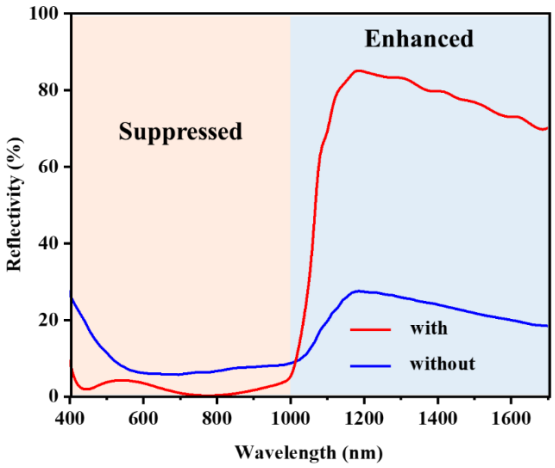

Fig. 4 The spectral reflectivity of the crystalline silicon photovoltaic cell with/without nanofilm reflector

The reflectivity of the crystalline silicon photovoltaic cell with two layers of TiO_2/SiO_2 nanofilm reflector under unpolarized, TE polarized and TM polarized state in the wavelength range of 400~2500 nm, as presented in Figs. 5(b)-(d). The unpolarized state is the arithmetic mean of TM and TE polarized state (unpolarized state = $\frac{TM+TE}{2}$). As shown in the figure, under unpolarized and TE polarized state, the reflectivity of the crystalline silicon photovoltaic cell with nanofilm reflector is insensitive to the angle in the 0° ~ 70°, which are lower than 10%. Under TM polarized state, the reflectivity of the crystalline silicon photovoltaic cell with nanofilm reflector is insensitive to the angle in the 0° ~ 60°, which are lower than 10%. The reflectivity of the crystalline silicon photovoltaic cell with nanofilm reflector increases with angle for 70° to 90° for all unpolarized, TE polarized and TM polarized state. Especially when the angle is above 85°, the reflectivity of the crystalline silicon photovoltaic cell with nanofilm reflector tends to 1. For the practice, the 85° irradiation will only occur when day and night alternate, and the irradiance at this time is usually very small. Therefore, when the angle is greater than 85°, although the reflectivity of a crystalline silicon photovoltaic cell with nanofilm reflector tends to 1, it has little effect on its daily power generation.

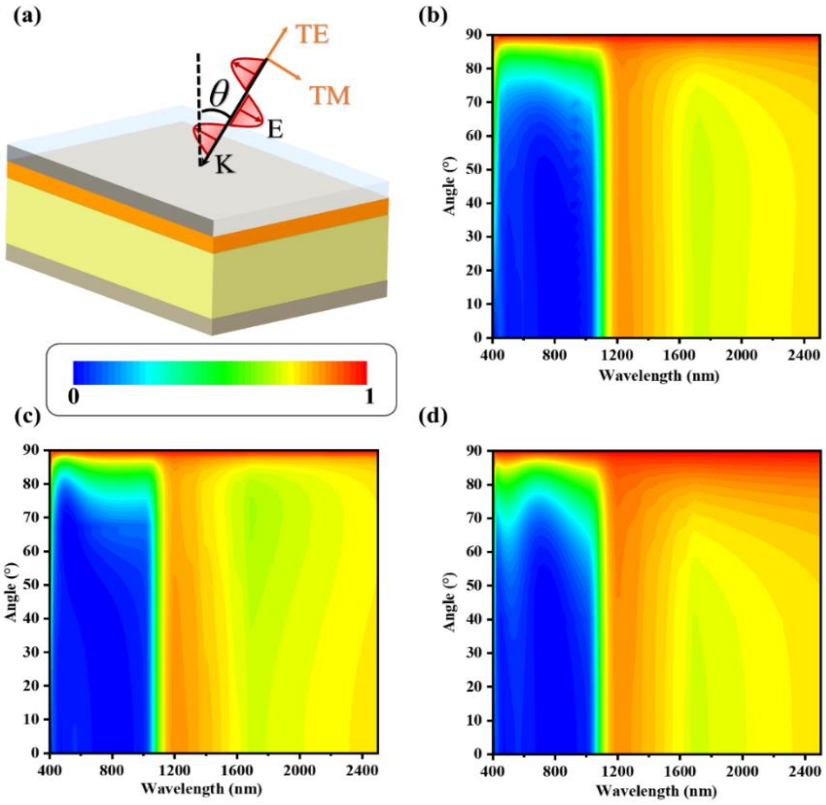

Fig. 5 (a) the effects of incident angle and polarization on the optical performance of the crystalline silicon photovoltaic cell with two layers of TiO_2/SiO_2 nanofilm reflector; (b) the reflectivity of PV with nanofilm reflector under unpolarized state; (c) the reflectivity of PV with nanofilm reflector under TE state; (d) the reflectivity of PV with nanofilm reflector under TM state

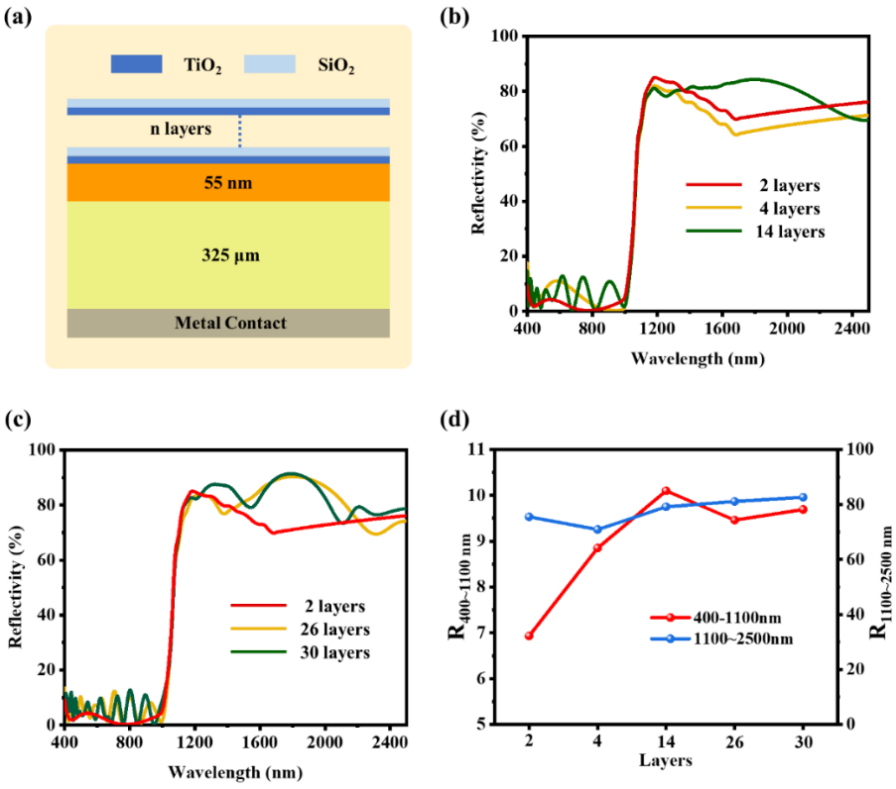

Fig. 6 (a) the effects of the number of layers on the spectral reflectivity; (b) the effects of 2, 4 and 14 layers on the spectral reflectivity; (c) the effects of 2, 26 and 30 layers on the spectral reflectivity; (d) the integral of reflectivity in 400~1100 nm and integral of reflectivity in 1100~2500 nm.

4.3 Number of layers study

Next, the effects of the number of layers on the spectral reflectivity of crystalline silicon photovoltaic cell with nanofilm reflector are investigated, as presented in Fig. 6 (a). Five different number of layers, 2 layers, 4 layers, 14 layers, 26 layers and 30 layers, are optimized while leaving the other parameters unchanged.

The effects of the number of layers on the spectral reflectivity of crystalline silicon photovoltaic cell with nanofilm reflector are shown in Figs. 6(b) and 6(c). As seen in the figures, the number of layers evidently influences the spectral reflectivity of crystalline silicon photovoltaic cell with nanofilm reflector at 400~2500 nm wavelengths. At 400~1100 nm wavelengths, the number of oscillating ripples increases with the increasement of the number of layers. The spectral reflectivity of crystalline silicon photovoltaic cell with nanofilm reflector is bellower than 5% when the number of layers is 2, while it is larger than 5% and fluctuates between 0 with 10% when the number of layers increases to 4 layers, 14 layers, 26 layers and 30 layers.

At 1100~2500 nm wavelengths, the number of oscillating ripples also increases with the increasement of the number of layers. The spectral reflectivity of crystalline silicon photovoltaic cell with nanofilm reflector fluctuates between 70%~85% when the number of layers is 2. The spectral reflectivity of crystalline silicon photovoltaic cell with 2 layers nanofilm reflector is about 5% higher than that of the crystalline silicon photovoltaic cell with 4 layers nanofilm reflector. However, the spectral reflectivity of crystalline silicon photovoltaic cell with 2 layers nanofilm reflector is lower than these of the crystalline silicon photovoltaic cell with 14, 26 and 30 layers nanofilm reflector, respectively.

The integral of reflectivity in 400~1100nm ($R_{400\sim1100nm}$) and integral of reflectivity in 1100~2500 nm ($R_{1100\sim2500nm}$) of crystalline silicon photovoltaic cell with nanofilm reflector are presented in Fig.6(d). As seen in the figure, the integral of reflectivity in 400~1100 nm ($R_{400\sim1100nm}$) of 2, 4, 14, 26 and 30 layers are 6.93%, 8.85%, 10.10%, 9.46% and 9.69%, respectively. The integral of reflectivity in 1100~2500 nm ($R_{1100\sim2500nm}$) of 2, 4,14, 26 and 30 layers are 69.73%, 75.51%, 70.91%, 79.15%, 81.11% and 82.65%, respectively. The integral of reflectivity in 400~1100 nm of crystalline silicon photovoltaic cell with 2 layers nanofilm reflector is only 6.93%, which is lower than those of crystalline silicon photovoltaic cell with 4, 14, 26 and 30 layers nanofilm reflector, respectively. The integral of reflectivity in 1100~2500 nm of crystalline silicon photovoltaic cell with 2 layers nanofilm reflector is 69.73%, which is not much weaker than those of crystalline silicon photovoltaic cell with 4 layers, 14 layers, 26 layers, and 30 layers, respectively. In addition to the integral of reflectivity, the authors also calculated the integral after multiplying reflectance and solar spectrum, and thus, the calculated results indicated that 20% of solar energy is reflected and 80% of solar energy is absorbed in the wavelength range of 400~2500 nm.

As mentioned above, a promising strategy is to allow crystalline silicon photovoltaic cell to absorb as much solar energy as possible from 400 to 1100 nm, while absorbing as little as possible from 1100 to 2500 nm. The integral of reflectivity in 400~1100 nm of crystalline silicon photovoltaic cell with 2 layers reflector is lower than those of crystalline silicon photovoltaic cell with 4,14, 26- and 30-layers reflector, respectively. Therefore, 2 layers reflector allow crystalline silicon photovoltaic cell to absorb as much solar energy as possible from 400 to 1100 nm. In addition, the integral of reflectivity in 1100~2500 nm of crystalline silicon photovoltaic cell with 2 layers reflector is almost same as those with 4,14, 26 and 30 layers nanofilm reflector. Furthermore, the 2 layers nanofilm reflector is easier to implement in terms of process manufacturing, and the cost is relatively low. Therefore, 2 layers nanofilm reflector is promising.

4.4 Conversion efficiency comparison

In this section, the effects of the nanofilm reflector on the temperature and energy conversion efficiency of crystalline silicon photovoltaic cell are investigated, as presented in Fig. 7. The nanofilm reflector is two layers, and the standard energy conversion efficiency of crystalline silicon photovoltaic cell under 25℃ is 20%. Figure 7(a) presents the temperature difference between the crystalline silicon photovoltaic cell and the ambient temperature (25°C). As seen in the figure, for crystalline silicon photovoltaic cell with 2 layers nanofilm reflector, the temperature differences are 13.71℃, 16.46℃, 19.20℃, 21.94°C, 24.69°C and 27.43°C when the solar irradiance are 500 W/m², 600 W/m², 700 W/m², 800 W/m², 900 W/m² and 1000 W/m², respectively. While for crystalline silicon photovoltaic cell without 2 layers nanofilm reflector, the temperature differences are 15.97℃, 19.16℃, 22.36℃, 25.55°C, 28.75°C and 31.94℃, when the solar irradiance is 500 W/m², 600 W/m², 700 W/m², 800 W/m², 900 W/m² and 1000 W/m², respectively. It can be found that the temperature of the crystalline silicon photovoltaic cell will increase with the increase of solar irradiance regardless of whether the nanofilm reflector is used or not. However, the temperature rises of crystalline silicon photovoltaic cell with 2 layers nanofilm reflector is smaller than that of crystalline silicon photovoltaic cell without 2 layers nanofilm reflector. To be precise, the use of nanofilm reflector can reduce the temperature of crystalline silicon photovoltaic cell by 2.26°C, 2.7°C, 3.16°C, 3.61°C, 4.06°C, 4.51°C, when the solar irradiance is 500 W/m², 600 W/m², 700 W/m², 800 W/m², 900 W/m², 1000 W/m², respectively.

The energy conversion efficiency of the crystalline silicon photovoltaic cell with and without 2 layers nanofilm reflector are presented in Fig. 7 (b). As seen in the figure, the energy conversion efficiency of the crystalline silicon photovoltaic cell with 2 layers nanofilm reflector are 18.84%,18.61%, 18.38%, 18.15%, 17.91% and 17.68%, when the solar irradiance is 500 W/m², 600 W/m², 700 W/m², 800 W/m², 900 W/m² and 1000 W/m², respectively. The energy conversion efficiency of the crystalline silicon photovoltaic cell without nanofilm reflector are 18.64%, 18.37%, 18.09%, 17.82%, 17.55% and 17.28%, when the

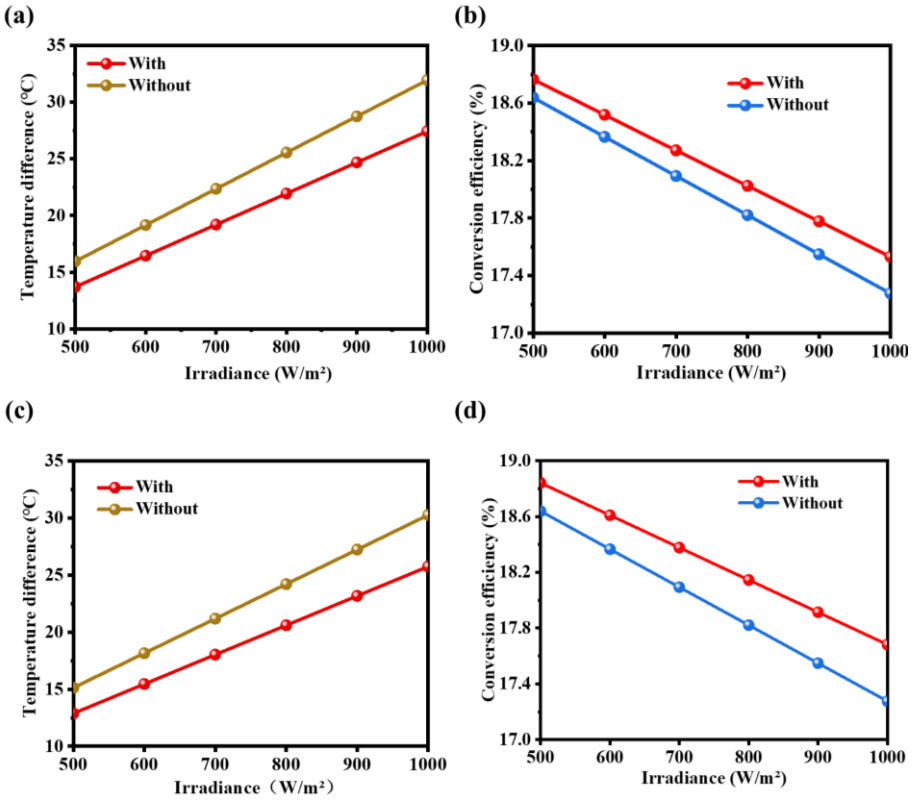

Fig. 7 (a) the temperature difference between the crystalline silicon photovoltaic cell with the ambient temperature (25℃) where the standard energy conversion efficiency is 20%; (b) the energy conversion efficiency between the crystalline silicon photovoltaic cell with and without nanofilm reflector; (c) the temperature difference between the crystalline silicon photovoltaic cell with the ambient temperature (25℃) where the standard energy conversion efficiency is 16.1%; (d) the energy conversion efficiency between the crystalline silicon photovoltaic cell with and without nanofilm reflector

solar irradiance is 500 W/m², 600 W/m², 700 W/m², 800 W/m², 900 W/m² and 1000 W/m², respectively. It can be found that the energy conversion efficiency of the crystalline silicon photovoltaic cell will decrease with the increase of solar irradiance regardless of whether the nanofilm reflector is used or not. This is because the temperature of photovoltaic cells increases with increasing solar irradiance. The energy conversion efficiency decreases of crystalline silicon photovoltaic cell using nanofilm reflector is smaller than that of crystalline silicon photovoltaic cell that does not use nanofilm reflector. To be precise, the use of nanofilm reflector can absolutely improve the energy conversion efficiency of crystalline silicon photovoltaic cell by 0.13%, 0.13%, 0.15%, 0.21%, 0.23% and 0.25%, when the solar irradiance is 500 W/m², 600 W/m², 700 W/m², 800 W/m², 900 W/m², 1000 W/m², respectively.

Next, the crystalline silicon photovoltaic cell with the standard energy conversion efficiency of 16.1% is selected, and the temperature differences and energy conversion efficiency of crystalline silicon photovoltaic cell are presented in Figs. 7(c) and 7(d). As seen in these figures, the similar trend of temperature and energy conversion efficiency could be obtained. It can be seen that, as long as the irradiance is the same, the temperature of crystalline silicon photovoltaic cell with nanofilm reflector is lower than that of crystalline silicon photovoltaic cell without nanofilm reflector, and the energy conversion efficiency of crystalline silicon photovoltaic cell with nanofilm reflector is higher than that of crystalline silicon photovoltaic cell without nanofilm reflector. In addition, the nanofilm reflector may be more practical in high irradiance environment.

5. Conclusions

Traditional cooling PV method based on solar spectrum regulation is using nanofluids or nanofilm-based spectral splitting devices, which are limited by precise optical path and high optical loss. In this paper, the idea of using nanofilm reflector to reduce the temperature of photovoltaic cells is proposed, which overcomes the limitation of high optical loss and precise optical path requirements existing in traditional cooling method based on solar spectrum regulation. Such nanofilm reflector is located on the surface of crystalline silicon photovoltaic cells to reflect sunlight wavelength with photon energy lower than the semiconductor band gap. In addition, such nanofilm reflector would not reflect sunlight wavelength with photon energy higher than the semiconductor band gap, which could maintain or even enhance the absorption of the

sunlight wavelength with photon energy higher than the semiconductor band gap for the crystalline silicon photovoltaic cells. The following conclusions can be drawn:

• the nanofilm reflector can reduce spectral reflectivity integral from 9.0% to 6.93% in 400~1100 nm wavelength range, and improve spectral reflectivity integral from 23.1% to 78.34% in 1100~1700 nm wavelength range;

• the nanofilm reflector can efficiently work for different sunlight's angle and polarization state;

• the nanofilm reflector can reduce the temperature of PV by 2.26°C, 2.7°C, 3.16°C, 3.61°C, 4.06°C, 4.51°C, when the solar irradiance is 500 W/m², 600 W/m², 700 W/m², 800 W/m², 900 W/m², 1000 W/m², respectively;

• the nanofilm reflector can improved the energy conversion efficiency of PV by 0.13%, 0.13%, 0.15%, 0.21%, 0.23% and 0.25%, when the solar irradiance is 500 W/m², 600 W/m², 700 W/m², 800 W/m², 900 W/m², 1000 W/m², respectively.

• In the future work, it is important to fabricated such 2 layers reflector, and conduct long-time stable test.

Acknowledgments

This work was supported by the National Natural Science Foundation of China Grant No. 52076064); Taishan Scholar Foundation of Shandong Province (tsqn201812 105).

References

Arıcı, M., Tükel, M., Yıldız, Ç., Li, D. and Karabay, H. (2020), "Is the thermal transmittance of air-filled inclined multi-glazing windows similar to that of vertical ones", *Energy Build*., **229**, 110515. https://doi.org/10.1016/j.enbuild.2020.110515.

Caselli, D., Liu, Z.C., Shelhammer, D. and Ning C.Z. (2014), "Composition-graded nanowire solar cells fabricated in a single process for spectrum-splitting photovoltaic systems", *Nano Lett*., **14**(10), 5772-5779. https://doi.org/10.1021/nl502662h.

Cote, B., Slauch, I., Deceglie, M., Silverman, T. and Ferry, V. (2021), "Light management in bifacial photovoltaics with spectrally selective mirrors", *ACS Appl*. *Energ*. *Mater*., **4**(6), 5397-5402. https://doi.org/10.1021/acsaem.1c01236.

Cheng, Z.M., Han. H., Wang, F.Q., Yan, Y.Y., Shi, X.H., Liang, H.X., Zhang, X.P. and Shuai, Y. (2021), "Efficient radiative cooling coating with biomimetic human skin wrinkle structure", *Nano Energy*, **89**, 106377. https://doi.org/10.1016/j.nanoen.2021.106377.

Daulet, S. (2021), "One-dimensional Schottky nanodiode based on telescoping polyprismanes", *Adv*. *Nano Res*., **10**(4), 339-347. https://doi.org/10.12989/anr.2021.10.5.471.

Evangelos, B., Christos, T. and Zafar, S. (2021), "Investigation and optimization of a solar-assisted pumped thermal energy storage system with flat plate collectors", *Energy Conv*. *Manag*., **237**, 114137. https://doi.org/10.1016/j.enconman.2021.114137.

Farideh, Y., Mehran, A. and Robert, A. (2020), "Numerical modeling of a concentrated photovoltaic/thermal system which utilizes a PCM and nanofluid spectral splitting", *Energy Conv*. *Manag*., **215**, 112927. https://doi.org/10.1016/j.enconman.2020.112927.

Fernandes, M.R. and Schaefer, L.A. (2021), "Levelized cost of energy of hybrid concentrating photovoltaic-thermal systems based on nanofluid spectral filtering", *Sol*. *Energy*, **227**, 126-136. https://doi.org/10.1016/j.solener.2021.08.041.

Green, M.A. (1995), "Silicon Solar Cells: Advanced Principles & Practice", University of New South Wales, Sydney, Australia.

Haviv, S., Revivo, N., Kruger, N., Manor, A., Khachatryan, B., Shustov, M. and Rotschild, C. (2020), "Luminescent solar power-PV/thermal hybrid electricity generation for cost-effective dispatchable solar energy", *ACS Appl*. *Mater*. *Interf*., **12**, 36040-36045. https://doi.org/10.1021/acsami.0c08185.

Huang. G. and Markides, C. (2021), "Spectral-splitting hybrid PV-thermal (PV-T) solar collectors employing semi-transparent solar cells as optical filters", *Energy Conv*. *Manag*., **248**, 114776. https://doi.org/10.1016/j.enconman.2021.114776.

Huang. J., Han. X.Y., Zhao. X.B. and Meng. C.F. (2021), "Facile preparation of core-shell Ag@SiO2 nanoparticles and their application in spectrally splitting PV/T systems", *Energy*, **215**(A), 119111. https://doi.org/10.1016/j.energy.2020.119111.

Hissouf, M., Feddaoui, M., Najim, M., Charef, A. and Kabeel, A.E. (2021), "Effect of optical, geometrical and operating parameters on the performances of glazed and unglazed PV/T system", *Appl*. *Therm*. *Eng*., **197**, 117358, https://doi.org/10.1016/j.applthermaleng.2021.117358.

Hu, M.K., Zhao, B., Suhendri, S., Cao, J., Wang, Q., Riffat, S., Yang, R., Su, Y. and Pei, G. (2022), "Experimental study on a hybrid solar photothermic and radiative cooling collector equipped with a rotatable absorber/ emitter plate", *Appl*. *Energ*, **306**, Part B, 118096. https://doi.org/10.1016/j.apenergy.2021.118096.

Ju. X., Xu. C., Liao. Z.R., Du. X.Z., Wei G.S., Wang. Z.F. and Yang. Y.P. (2017), "A review of concentrated photovoltaic-thermal (CPVT) hybrid solar systems with waste heat recovery (WHR)", *Sci*. *Bull*., **62**(20), 1388-1426. https://doi.org/10.1016/j.scib.2017.10.002.

Khan, S.B., Zhang, Z.J. and Lee, S.L. (2020), "Single component: bilayer TiO_2 as a durable antireflective coating", *J Alloy*. *Compd*., **834**, 155137. https://doi.org/10.1016/j.jallcom.2020.155137.

Kruitwagen, L., Story, K.T., Friedrich, J., Byers, L., Skillman, S., and Hepburn, C. (2021), "A global inventory of photovoltaic solar energy generating units", *Nature*, **598**, 604-610. https://doi.org/10.1038/s41586-021-03957-7.

Klaus, J., Peter, T., Eugene, A.K. and Christiane, B. (2021), "Perovskite/silicon tandem solar cells: Effect of luminescent coupling and bifaciality", *Sol*. *RRL*, **5**(3), 2000628. https://doi.org/10.1002/solr.202000628.

Lee, S.H. and Lee J.Y. (2018), "Homo-tandem structures to

achieve the ideal external quantum efficiency in small molecular organic solar cells", *Opt. Express*, **26**, A697-A708. https://doi.org/10.1364/OE.26.00A697.

Li. H.R., He. Y.R., Wang. C.H., Wang. X.Z. and Hu. Y.W. (2019), "Tunable thermal and electricity generation enabled by spectrally selective absorption nanoparticles for photovoltaic/thermal applications", *Appl. Energy*, **236**, 117-126. https://doi.org/10.1016/j.apenergy.2018.11.085.

Liang, H.X., Wang, F.Q., Zhang, D., Cheng, Z.M., Zhang, C.X., Lin, B. and Xu, H.J. (2020), "Experimental investigation of cost-effective ZnO nanofluids based spectral splitting CPV/T system", *Energy*, **194**, 116913. https://doi.org/10.1016/j.energy.2020.116913.

Liang. S., Zheng. H.F., Ma. X.L., Liu. F.Z., Wang. G. and Zhao. Z.Y. (2021), "Study on a passive concentrating photovoltaic-membrane distillation integrated system", *Energ Convers. Manage*., **242**, 114332. https://doi.org/10.1016/j.enconman.2021.114332.

Michel, C., Blain, P., Clermont, L., Languy, F., Lenaerts, C., Fleury-Frenette, K., Décultot, M., Habraken, S., Vandormael, D., Cloots, R., Thalluri, G.K.V.V., Henrist, C., Colson, P. and Loicq, J. (2017), "Waveguide solar concentrator design with spectrally separated light", *Sol. Energy*, **157**, 1005-1016. https://doi.org/10.1016/j.solener.2017.09.015.

Mateusz, J., Topias, S., Lauri, U., Harm, O. and Mikael, R. (2018), "Effective modelling of borehole solar thermal energy storage systems in high latitudes", *Geomech. Eng*., **16**(5), 503-512. https://doi.org/10.12989/gae.2018.16.5.503.

Muhammad, J., Shazia, A., Amir, W., Faiz, R., Bilal, A., Muhammad B. and Ahson J. (2019), "Plasmonic effects and size relation of gold-platinum alloy nanoparticles", *Adv. Nano Res*., **7**(3), 169-180. https://doi.org/10.12989/anr.2019.7.3.169.

Otanicar, T., Dale, J., Orosz, M., Brekke, N., DeJarnette, D., Tunkara, E., Roberts, K. and Harikumar, P. (2018), "Experimental evaluation of a prototype hybrid CPV/T system utilizing a nanoparticle fluid absorber at elevated temperatures", *Appl. Energ*, **228**, 1531-1539. https://doi.org/10.1016/j.apenergy.2018.07.055.

Qiu, Y., Zhang, P.F., Li, Q., Zhang, Y.T. and Li, W.H. (2021), "A perfect selective metamaterial absorber for high-temperature solar energy harvesting", *Sol. Energ*, **230**, 1165-1174. https://doi.org/10.1016/j.solener.2021.11.034.

Qiao, Y., Yousef, Z., Abouzar, R., Sara, P., Angel, R., Mohamed, A., Mohammed, J., Ehsan, K. and Hamid, A. (2021), "Nano-SiO_2 for efficiency of geotechnical properties of fine soils in mining and civil engineering", *Adv. Nano Res*., **11**(3), 301-312. https://doi.org/10.12989/anr.2021.11.3.301.

Robert, A., Todd, O. and Gary, R. (2012), "Nanofluid-based optical filter optimization for PV/T systems", *Light Sci. Appl*., **1**, 34. https://doi.org/10.1038/lsa.2012.34.

Ravi, S. and Vivek, B. (2021), "Recent advances in ZnO nanostructures and their future perspective", *Adv. Nano Res*., **11**(1), 37-54. https://doi.org/10.12989/anr.2021.11.1.037.

Santbergen, R. and Zolingen, R. (2008), "The absorption factor of crystalline silicon PV cells: A numerical and experimental study", *Sol. Energy Mater. Sol. Cells*, **92**, 432-444. https://doi.org/10.1016/j.solmat.2007.10.005.

Slauch, I., Deceglie, M., Silverman, T. and Ferry, V. (2018), "Spectrally selective mirrors with combined optical and thermal benefit for photovoltaic module thermal management", *ACS Photonics*, **5**(4), 1528-1538. https://doi.org/10.1021/acsphotonics.7b01586.

Tikhonravov. A.V., Trubetskov. M.K., and DeBell. G.W. (1996), "Application of the needle optimization technique to the design of optical coatings", *Appl. Opt*., **35,** 5493-5508. https://doi.org/10.1364/AO.35.005493.

Taylor, S., Long, L., McBurney, R., Sabbaghi, P., Chao, J. and Wang, L. (2020), "Spectrally-selective vanadium dioxide based tunable metafilm emitter for dynamic radiative cooling", *Sol. Energy Mater. Sol. Cells*, **e217**, 110739. https://doi.org/10.1016/j.solmat.2020.110739.

Zarmai, M.T., Ekere, N.N., Oduoza, C.F. and Amalu, E.H. (2015), "A review of interconnection technologies for improved crystalline silicon solar cell photovoltaic module assembly", *Appl. Energ*, **154**, 173-182. https://doi.org/10.1016/j.apenergy.2015.04.120.

Zhang. X., Lei. D.Q., Zhang. B., Yao. P. and Wang. Z.F. (2021), "SiN_x/Cu spectral beam splitting films for hybrid photovoltaic and concentrating solar thermal systems", *ACS Omega*, **6**(33), 21709-21718 https://doi.org/10.1021/acsomega.1c03178.

Zhang, C.X., Shen, C., Zhang, Y.B. and Pu, J.H. (2022), "Feasibility investigation of spectral splitting photovoltaic/ thermal systems for domestic space heating", *Renew Energ*, **192**, 231-242. https://doi.org/10.1016/j.renene.2022.04.126.

JL